

Time dependent IRM acquisition as a tool to quantify the abundance of ultrafine superparamagnetic magnetite in loessic soils

Tamara A. Machac,¹ C. William Zanner² and Christoph E. Geiss¹

¹Department of Physics, Trinity College, 300 Summit St., Hartford, CT 06106, USA. E-mail: christoph.geiss@trincoll.edu

²Department of Soil, Water and Climate, University of Minnesota, 1991 Upper Buford Circle, St. Paul, MN 55108, USA

Accepted 2007 January 10. Received 2007 January 9; in original form 2006 August 9

SUMMARY

The time dependence of Isothermal Remanent Magnetization acquisition (tIRM) is a rapid, sensitive and inexpensive way to quantify the presence of ultrafine ferrimagnetic grains straddling the superparamagnetic–single domain grain size boundary, well suited for use in small rock magnetic laboratories. The technique is very selective to the presence of grains with a diameter of approximately 25 nm, and tIRM results correlate well with measurements of frequency dependent susceptibility without the need of correcting for the presence of paramagnetic minerals. A simple IRM acquisition model can be used to obtain quantitative abundance estimates for these ultrafine magnetic grains. Application of tIRM measurements to eleven soil profiles from the Midwestern United States shows that the abundance of ultrafine particles increases with precipitation, as long as the mean annual precipitation is below 850 mm a⁻¹. Sites that developed under more humid conditions show a decrease in tIRM and likely SP abundance, probably caused by increased iron reduction and translocation during more common periods of reducing conditions.

Key words: Climate, laboratory measurements, magnetic domains, magnetite, remanent magnetization.

INTRODUCTION

Magnetic grains in soils and sediments can record palaeomagnetic variations in the Earth's magnetic field, as well as changes in the palaeoclimate and palaeo-environment (e.g. Reynolds & King 1995; Oldfield *et al.* 2003; Deng *et al.* 2005). Climatic change affects the environments in which sediments and soils form. This then leads to changes in soils' magnetic mineralogy, concentration, grain size and morphology (e.g. Bloemendal *et al.* 1992; Geiss *et al.* 2003; Spassov *et al.* 2005).

Studies of Chinese loess and palaeosols show a significant correlation between magnetic susceptibility, the deep-sea oxygen isotope record, and climate changes (e.g. Kukla *et al.* 1988; Heller & Evans 1995; Maher & Thompson 1999). The analyzed Chinese palaeosols contain higher concentrations of single domain (SD), as well as superparamagnetic (SP) ultrafine-grained magnetite (e.g. Maher & Thompson 1992; Banerjee *et al.* 1993; Kletetschka & Banerjee 1995; Porter *et al.* 2001). Soil wetness and temperature determine the formation and preservation of ultrafine-grained magnetite during soil formation, especially in the upper soil horizons (Maher & Taylor 1988; Maher & Thompson 1992; Dearing *et al.* 1996b; Han *et al.* 1996). SP particles are most likely created through weathering of weakly magnetic iron-bearing minerals and production of ferrihydrite as an intermediate phase. Fe reduction, which is often bacterially mediated, can then lead to the formation of magnetite, which may partially oxidate to maghemite over time (Dearing *et al.*

1996b; Singer *et al.* 1996). Studies of various English soils show that weathering, geological and soil processes, rather than burning, pollution and land use, are the dominant influence on the magnetic properties of topsoils (Dearing *et al.* 1996b, 1986). Such findings provide links between the magnetic properties of soils and the environmental conditions under which they have formed, and several studies (Heller & Liu 1986; Heller *et al.* 1993; Maher *et al.* 1994; Sartori *et al.* 2005) attempted to use the magnetic properties of paleosols to reconstruct past climatic conditions. Often, erosion caused by agricultural practices and land clearing, removes the magnetically enhanced horizon and results in magnetically depleted soils (Dearing *et al.* 1986; Maher & Thompson 1992). If the magnetic signal of these lost soil horizons is sufficiently well known it is possible to track the eroded sediment into streams and lakes and create a record of soil erosion through time based on the magnetic properties of lake or even marine sediment (Dearing *et al.* 2001; Dearing & Jones 2003). The success of such studies requires careful characterizations of the soils' initial magnetic properties. Most pedogenic magnetite is fine grained (e.g. Hunt *et al.* 1995), therefore, we need techniques that easily and rapidly recognize and quantify such fine grains in a large number of samples.

Current techniques to detect fine-grained, SP ferromagnetic minerals involve the determination of frequency dependent susceptibility (χ_{fd}) (e.g. Dearing *et al.* 1996a; Forster *et al.* 1994; Worm 1998) or the controlled dissolution of the ultrafine magnetic component through citrate–bicarbonate–dithionite (CBD) treatment (e.g. Hunt

et al. 1995; Vidic et al. 2000). Frequency dependent susceptibility is not a reliable parameter for detecting changes in the quantity of SP material, especially in natural samples containing a mixture of magnetic phases. It requires correction for the presence of paramagnetic minerals, which is rarely done, and is difficult to measure for weakly magnetized samples.

Our study expands on work by Worm (1999) which showed that measurements of the time dependence of Isothermal Remanent Magnetization acquisition (tIRM) and frequency dependent susceptibility measurements (χ_{fd}) give nearly equivalent information about particles straddling the SP–SD grain size boundary. We investigate this alternative inexpensive, fast and sensitive method to detect and quantify the abundance of very small grains near the superparamagnetic–stable single domain (SP–SSD) boundary in natural soil samples. The abundance of ultrafine magnetic grains (diameter smaller than 20 nm) in soils is thought to vary with changes in climate, especially precipitation and we test this hypothesis by relating our quantitative results for modern loessic soils to changes in present day precipitation in the Midwestern United States.

BACKGROUND AND METHODS

An IRM measurement of an assemblage of grains spanning the SP–SSD grain size boundary can be treated as a sample approaching an equilibrium magnetization in an external field B_{ext} , followed by viscous decay during the actual remanence measurement in zero field (Dunlop & Özdemir 1997; Worm 1999). IRM acquisition in an external magnetic field B_{ext} can be described as:

$$M(t) = M_{\text{eq}} - (M_{\text{eq}} - M_0) e^{-\frac{t}{\tau}}, \quad (1)$$

where M_{eq} is the equilibrium magnetization of an assemblage of SP grains, M_0 is the initial magnetization ($M_0 = 0$ for an initially demagnetized sample), t_{mag} is the time the sample is exposed to a magnetic field, and τ is the relaxation time (eq. 8.17 in Dunlop & Özdemir 1997). During remanence acquisition the equilibrium magnetization is given by

$$M_{\text{eq}} = n\mu L(\alpha), \quad (2)$$

where n is the number of particles per unit volume (V), $\mu = M_s V$ is the magnetic moment of each individual particle, L is the Langevin function [$L(x) = \coth(x) - 1/x$], and $\alpha = (\mu_r B_{\text{ext}})/(kT)$ is the ratio between the magnetic and thermal energies. Since the actual measurement of the acquired IRM takes some time the magnetic remanence will undergo viscous decay in (near) zero magnetic field, described as

$$M_r = M_0 e^{-\frac{t_{\text{meas}}}{\tau(B=0)}}, \quad (3)$$

where M_0 is the previously acquired magnetization, t_{meas} is the time required for a measurement and τ is the relaxation time for $B_{\text{ext}} = 0$. Combining eqs (1) and (2) shows that the measured IRM depends on the magnetization time t_{mag} and the measurement time t_{meas} , as well as the grain size of the SP grains under consideration (due to the volume-dependence of τ and α). We obtain for the measured IRM

$$IRM_{\text{measured}} = n\mu L(\alpha) \left(1 - e^{-\frac{t_{\text{mag}}}{\tau(B=B_{\text{ext}})}}\right) e^{-\frac{t_{\text{meas}}}{\tau(B=0)}}. \quad (4)$$

We employ a simple coil arrangement (Worm 1999) that allows us to expose samples to a weak magnetic field ($B_{\text{ext}} \approx 2$ mT) for controlled time intervals t_{mag} . The exact value of B_{ext} is not critical,

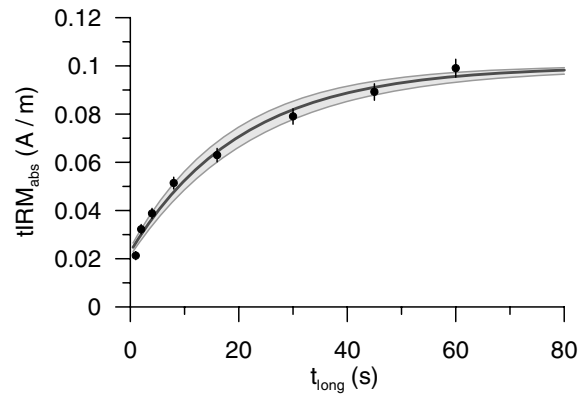


Figure 1. $tIRM_{\text{abs}}$ values for a short-acquisition time $t_{\text{short}} = 0.02$ s and values of t_{long} . Ranging between 1 and 60 s. Solid black line is the best fit to the data. Light grey area represents the estimated error of the fit. For more information on error estimation see text.

but the magnetizing field should be fairly low as tIRM values will be maximized for small magnetizing fields (Worm 1999). Dropping the sample through the coil briefly exposes it to a magnetic field for approximately 0.02 s. Longer magnetization times can be achieved by simply placing the sample into the coil for the required length of time. The tIRM acquisition can be expressed as the absolute difference between the two IRM measurements, which reflects the absolute abundance of particles contributing to tIRM

$$tIRM_{\text{abs}} = IRM_{\text{long}} - IRM_{\text{short}}. \quad (5)$$

If we are interested in the relative abundance of these particles normalized tIRM might be useful:

$$tIRM_{\text{rel}} = (IRM_{\text{long}} - IRM_{\text{short}})/IRM_{\text{long}}. \quad (6)$$

From eqs (1)–(4) it is clear that, aside from the details of the IRM measurement ($t_{\text{meas}}, B_{\text{ext}}$), $tIRM_{\text{abs}}$ depends on the particle size distribution (IRM depends on τ which itself depends on the particle volume V), the number of particles spanning the SP–SSD boundary per unit volume (n) and the two acquisition times t_{short} and t_{long} . Keeping t_{short} constant and measuring $tIRM_{\text{abs}}$ as a function of t_{long} it is possible to obtain estimates for the affected particle diameter (d) and the abundance of grains contributing to $tIRM_{\text{abs}}$. For our calculations we assume spherical grains with $V = 4/3\pi(0.5d)^3$, though assuming other simple grain shapes (e.g. cubic grains with $V = d^3$) makes little difference. Fig. 1 shows measurements of $tIRM_{\text{abs}}$ as a function of t_{long} for a soil sample from the Iowa loess hills. Numerical values for n and d are most easily found by trial and error, which is simplified by the fact that the critical grain diameter that contributes most to tIRM is closely centred around 25 nm. This narrow grain size window is due to the exponential dependence of τ on the particle volume V and our choice of IRM acquisition times (t_{short} and t_{long}) and the IRM acquisition field (B_{ext}). We employed a Monte Carlo algorithm that randomized values of n , d and an offset parameter $tIRM_0$ and calculated the standard deviation between the measured data and eq. (5), repeating the procedure 200 000 times. To estimate the error of our fitting procedure we averaged values for n , d and $tIRM_0$ for the best 20 fits. The resulting range of fits is shown in light grey. The offset parameter $tIRM_0$ attempts to address all non-SP contributions to the observed viscous acquisition and decay processes.

Having obtained values of d and n it is now possible to estimate the total abundance of particles straddling the SP–SSD boundary and compare it to the total volume of magnetic grains present in the sample. Assuming magnetite as the main carrier of magnetization we obtain the volume of semi-stable SP particles

$$V_{SP} = n \frac{4}{3} \pi \left(\frac{1}{2} d \right)^3 V_{\text{sample}}, \quad (7)$$

where V_{sample} is the volume of the measured sample. The total volume of the magnetic fraction (V_{mag}) can be obtained from hysteresis measurements. It is given by

$$V_{\text{mag}} = \frac{J_S}{M_S}, \quad (8)$$

where J_S is the saturation moment of the sample (in Am^2) and M_S is the saturation magnetization of magnetite ($M_S = 480 \text{ kA m}^{-1}$). Eqs (7) and (8) can be used to estimate the abundance of particles contributing to tIRM.

We measured magnetic remanence after exposing the sample to a weak magnetic field ($B_{\text{ext}} = 2 \text{ mT}$) for the desired length of time using an AGICO JR6 Spinner magnetometer. To standardize the remanence measurement and reduce the duration of the measurement samples were measured in one position only. The signal of the empty sample holder is about two orders of magnitude smaller than the weakest IRM measurement and we corrected for its presence by measuring the empty holder prior to each series of measurements and by subtracting the holder signal from each remanence measurement. To arrive at a reproducible initial state every sample was demagnetized in an alternating magnetic field of 300 mT peak amplitude prior to remanence acquisition. The demagnetization was performed using a Magnon International AFD300 alternating field demagnetizer. Sample errors were estimated by repeatedly measuring a subset of samples and calculating averages and standard deviations for these repeated measurements. Based on these measurements we estimated a relative error of 10 per cent for remanences smaller than 10^{-2} A m^{-1} and a relative error of 5 per cent for remanences larger than 10^{-2} A m^{-1} . The described procedure offers a compromise between speed of measurement, which is an important consideration when measuring viscous effects, and necessary precision. In our laboratory it takes about 60 s to remove the sample from the magnetizing field, mount it in the sample holder and complete a measurement. t_{meas} will depend on the laboratory setup used, but fortunately its absolute value is not critical as long as it stays within reasonable limits of a minute or so and is kept as constant as possible from measurement to measurement.

Our tIRM measurements were compared to standard measurements of frequency dependent susceptibility (χ_{fd}) measured using a Bartington susceptibility meter equipped with a MS2B dual-frequency sensor. Susceptibility was measured at 465 Hz (χ_{lf}) and 4.65 kHz (χ_{hf}) and frequency dependent susceptibility was calculated as

$$\chi_{fd} \text{ (in per cent)} = \frac{(\chi_{lf} - \chi_{hf})}{\chi_{lf}} \times 100. \quad (9)$$

Repeated measurements of χ_{fd} for the same sample allowed us to estimate errors for χ_{fd} .

We applied our method to loessic soils from the Midwestern United States where we sampled profiles of well-preserved modern soils from undisturbed sites across Nebraska, Iowa and Missouri that developed in Peoria Loess (Bettis *et al.* 2003). Soil cores were collected using a hydraulic soil probe, samples for magnetic analyses were air-dried, gently crushed by hand, sieved through a

2 mm-sieve and packed into weakly diamagnetic plastic boxes of 5.3 cm^3 volume. A detailed soil description and the magnetic properties of one representative site have been reported previously by Geiss *et al.* (2004). The correlation between magnetic properties and present-day climate has been described in a more recent paper (Geiss and Zanner, in press), which also contains soil descriptions and magnetic property variations for four representative sites across our transect.

RESULTS AND DISCUSSION

Reproducibility of tIRM measurements

To test the reproducibility of our tIRM measurements we performed repeated measurements on one sample, DBO 03-A 15 cm. Fig. 2 summarizes the results of these measurements. Samples DBO03-A 1 and DBO03-A 2 are fresh samples from the same soil horizon that have not been exposed to any laboratory-induced magnetic field prior to our tIRM experiments. Initial tIRM_{rel} measurements of these two samples have similar values of tIRM_{rel}. We then AF-demagnetized sample DBO03-A 1 in a 25 mT peak field and re-measured tIRM_{rel}. The value of this repeat-measurement is much higher than the original. Clearly, the applied peak field of 25 mT is not sufficient to remove the previous IRM acquisition history, even though the previously applied IRM acquisition field is much lower ($B_{\text{ext}} = 2 \text{ mT}$). To remove any previous IRM acquisition history we repeatedly demagnetized sample DBO03-A 2 in a 300 mT AFD field and re-measured tIRM_{rel}. All of these measurements yield tIRM_{rel} results that are lower than the original measurement, but have fairly similar values. Demagnetizing sample DBO 03A-1 in a peak field of 300 mT yields tIRM values consistent with the results obtained for DBO 03A-2. The same is true for a fresh sample (DBO03-A 3), which was demagnetized in a 300 mT field before the first tIRM measurement. Our results show that the numerical values of tIRM depend on the initial state of the sample, but that demagnetization in a strong alternating field ($B_{\text{peak}} = 300 \text{ mT}$) provides reproducible starting conditions, which lead to highly reproducible values for tIRM.

Comparison of tIRM and frequency dependent susceptibility measurements

Presently, tIRM measurements are not a widely used technique for the estimation of the SP component. Worm (1999) compares tIRM measurements performed on a wide range of samples, and we extend his data by comparing tIRM measurements with conventional measurements of χ_{fd} obtained with a Bartington dual frequency sensor. Our soil samples come from a soil core taken at Daniel Boone Conservation Area in central Missouri (Geiss and Zanner, in press), which shows a wide range of tIRM and χ_{FD} values. The results are presented in Fig. 3, and it is clear that both measurements characterize a very similar grain size fraction of the sample as both measurements yield roughly equivalent results. All χ_{fd} values shown in Fig. 3 have been corrected for paramagnetic contributions to χ by calculating the paramagnetic susceptibility (χ_p) from hysteresis measurements and subtracting it from the low-field susceptibility χ prior to calculating χ_{fd} . Error bars were obtained from an average of five χ_{fd} and three tIRM_{rel} measurements. The best-fitting line indicates a very good correlation between these two parameters ($r^2 = 0.98$). Our other Midwestern soil sites follow this correlation with χ_{fd} as well (data not shown).

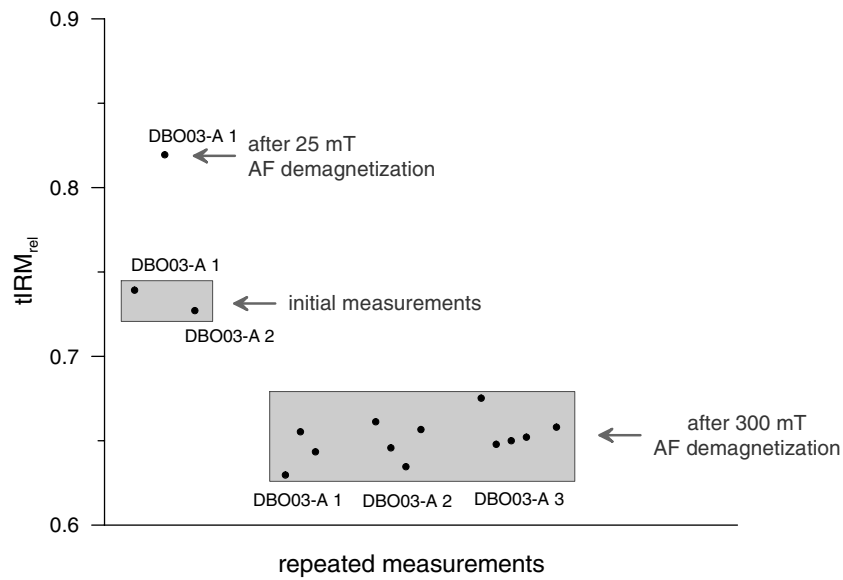


Figure 2. Repeated measurements of tIRM for three samples from Daniel Boone Conservation Area (DBO 03-A 15–20 cm). All samples come from one homogenized batch of soil and have not been subjected to any laboratory induced magnetic fields prior to the tIRM measurement. The initial measurement of samples A1 and A2 show the precision of the tIRM analysis. Sample A1 was remeasured after alternating field demagnetization in 25 mT and yielded a significantly higher tIRM measurement. Only after AF demagnetization in a relatively high field (300 mT) are all samples in a comparable domain state which enables repeatable tIRM measurements.

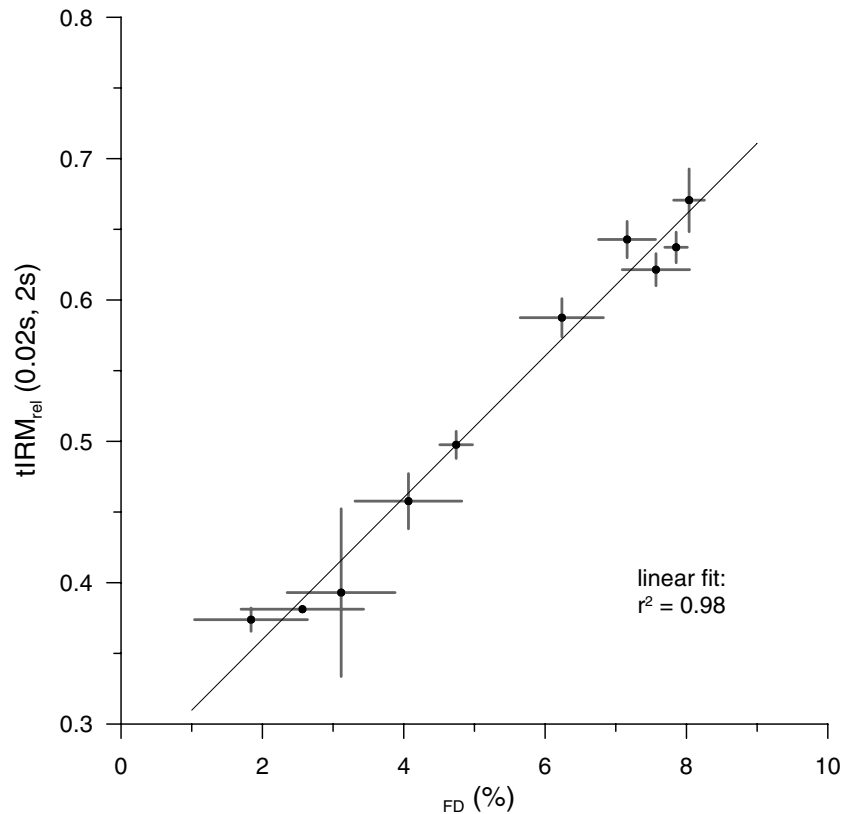


Figure 3. Comparison between tIRM measurements and measurements of frequency dependent susceptibility χ_{fd} shows good correlation between the two measurements.

Influence of magnetization time t_{long}

As shown earlier it is possible to estimate the volume fraction of the fine-grained magnetic component (f_{SP}) by measuring tIRM_{rel}

while varying t_{long} . This approach, however, is tedious and time consuming, and we wonder whether it is possible to estimate f_{SP} from one tIRM_{rel} measurement alone and whether there is an optimum t_{long} value. Fig. 4 shows tIRM_{rel} values as a function of f_{SP} for three

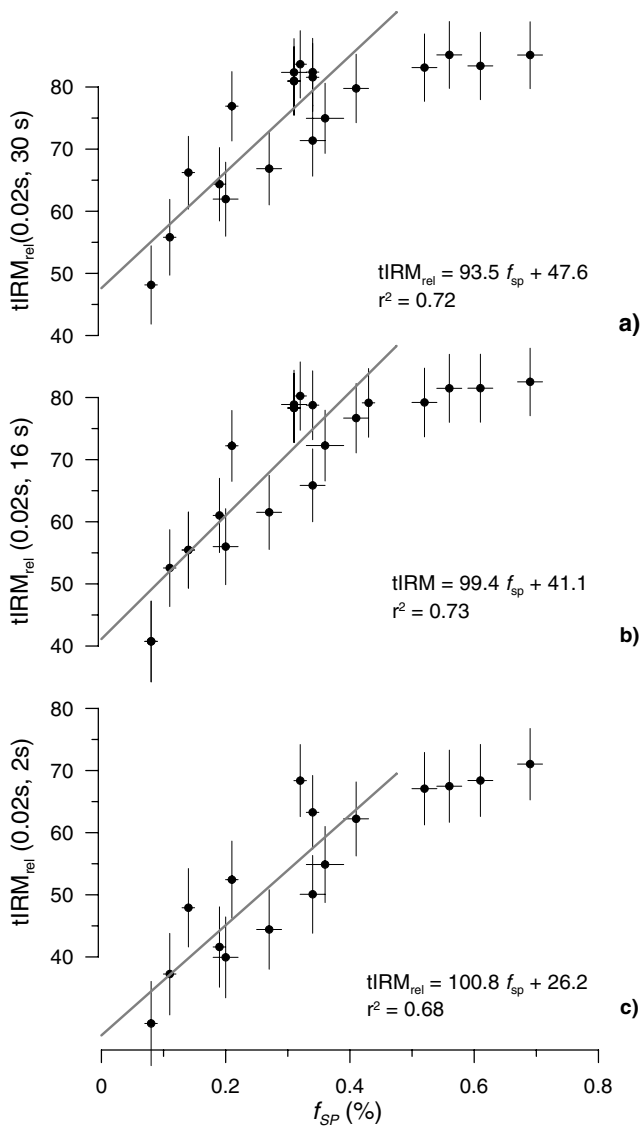


Figure 4. Correlation between tIRM measurements and the abundance of the superparamagnetic component f_{SP} for three values of t_{long} . The three sets of measurements are nearly identical, suggesting that within a reasonable range the exact value of t_{long} is not relevant.

values of t_{long} (2, 16 and 30 s). For $f_{SP} < 0.5$ per cent we find a good correlation between $tIRM_{rel}$ and f_{SP} for all curves, which allows us to roughly estimate f_{SP} from a single tIRM measurement using the correlations between $tIRM_{rel}$ and f_{SP} shown in Figs 4(a)–(c). All curves, however, tend to flatten out for $f_{SP} > 0.5$ per cent, making it difficult to estimate f_{SD} for samples containing higher concentrations of ultrafine material. In theory, this early saturation might seem like a severe limitation of the tIRM method. One should keep in mind, however, that tIRM measurements are sensitive to a rather small grain size window only (centred around 25 nm), which tends to result in small numerical values for f_{SP} . It would be interesting to test the method for finer grained lake sediments, which can have χ_{fd} values up to 15 per cent (Geiss & Banerjee 1997) which suggests correspondingly higher values of f_{SP} .

Since there is very little difference between Figs 4(a)–(c) we can choose any convenient value for t_{long} . Most of the measurements for this study are performed with $t_{long} = 2$ s because they were

performed before we investigated the role of t_{long} , and we chose t_{long} to be two orders of magnitude longer than t_{short} . In our laboratory we now prefer $t_{long} \approx 10$ s. Shorter times are difficult to maintain accurately, while longer time periods add to the tedium of measuring large sample sets.

tIRM in soils as a potential precipitation proxy

In Fig. 5, we apply our tIRM method to a series of modern soils from the Midwestern US and plot $tIRM_{rel}$ ($t_{long} = 2$ s) as a function of depth for 11 soil profiles. All sites have enhanced $tIRM_{rel}$ values in the upper soil horizons, indicating an increase in the relative abundance of ultrafine ferrimagnetic material in the upper soil horizons. The increase is modest for soils that developed under relatively dry conditions (Figs 5a–c) and more pronounced for soils that developed under more humid conditions (Figs 5d–k). To further quantify the relative change in ultrafine ferrimagnetic minerals as a function of mean annual precipitation we define the change in $tIRM_{rel}$ for each soil site as

$$\Delta tIRM_{rel} = \frac{tIRM_{max} - tIRM_{parent}}{tIRM_{parent}}, \quad (10)$$

where $tIRM_{max}$ is the maximum $tIRM_{rel}$ value measured in the profile, and $tIRM_{parent}$ is the average $tIRM_{rel}$ value for the (presumably) unaltered parent material. Fig. 6 compares this change in $tIRM_{rel}$ with mean annual rainfall for each site shown in Fig. 5. There appears to be a fairly good positive correlation between precipitation and the relative abundance of ultrafine ferrimagnetic minerals present in the upper soil horizons for soils that developed under dry to moderately humid climatic conditions. This correlation breaks down for the three wettest sites (HON03-A, DBO03-A and DAV03-A). Here, the graph flattens out, which may be due to the saturation effects as seen in Fig. 4 or due to an increased dissolution of ultrafine ferrimagnetic grains. As mean annual rainfall increases towards the eastern end of our transect sites, at some point, are more likely to experience periodic reducing conditions which lead to the removal of iron oxide minerals. Such reductive losses have been suggested for more humid soils and observed for the Eemian paleosol at Dolní Vonice, Czech Republic (Oches & Banerjee 1996) and for numerous modern Chinese soils by Han *et al.* (1996).

When using magnetic parameters to reconstruct past climatic soil-forming conditions we prefer relative measures of change because they may be better suited to deal with changes in the underlying parent material (Geiss & Zanner 2007). If a measure of absolute change is preferred it is possible to use the unnormalized difference in tIRM between the parent material and the magnetically enhanced topsoil.

CONCLUSIONS

The time dependence of IRM is a reliable and inexpensive alternative to frequency dependent susceptibility when estimating the abundance of SP particles in natural samples. The low cost of the needed equipment, the fact that all measurements are conducted at room temperature and can be performed using a simple spinner magnetometer make the technique well suited for small magnetic laboratories. Since the technique is based on measurements of magnetic remanence, it is easier to interpret than frequency dependent susceptibility, which needs to be corrected for the presence of paramagnetic minerals.

Because initial sample conditions greatly influence the outcome of the measurement, we recommend demagnetizing the sample in

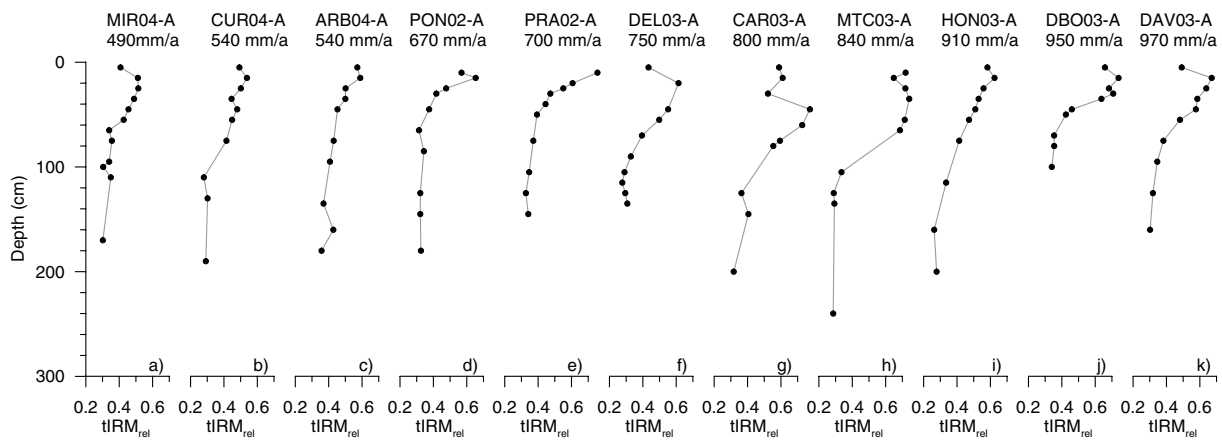


Figure 5. Application of the tIRM technique to samples from eleven loessic soil profiles from the Midwestern United States. Samples are arranged in order of increasing mean annual precipitation. For more information on soil profiles see (Geiss and Zanner, in press).

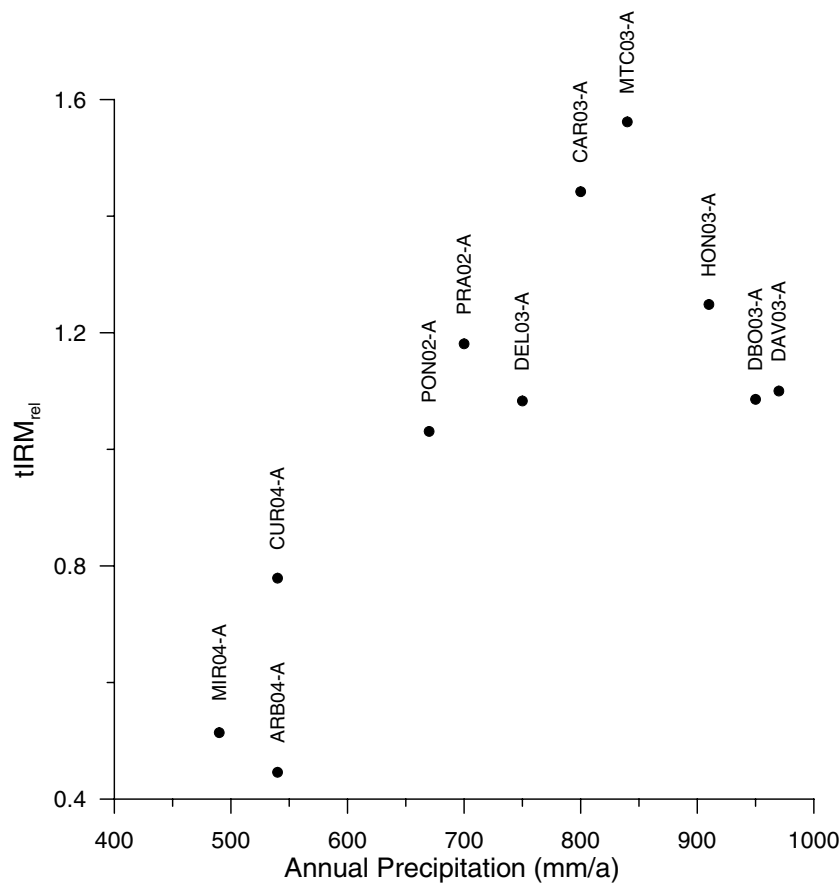


Figure 6. Normalized tIRM difference between magnetically enhanced topsoil and pedogenically unaltered parent material. Soils that develop under dry to moderately humid conditions show an increase in tIRM (and hence the abundance of ultrafine ferrimagnetic grains) with mean annual precipitation. This relationship breaks down for soils that formed under humid conditions.

a relatively high (200–300 mT) alternating magnetic field before measuring.

To aid in the interpretation of tIRM measurements we developed a simple model which allows for quantitative estimates of the abundance of ultrafine ferrimagnetic minerals straddling the SP–SSD boundary. By varying the IRM acquisition time t_{long} , we are able to quantify the relative abundance of ultrafine ferrimagnetic grains in the SP–SD boundary. Since this method is somewhat tedious, it is

possible to obtain a rough abundance estimate based on one tIRM measurement using the relationships between $tIRM_{rel}$ and f_{SP} given in Fig. 4. With our analyses being limited to loessic soils from the Midwestern United States, we recommend, however, verifying this relationship between tIRM and f_{SP} for a few samples from any new sites before using this simplified approach.

Fig. 4 also shows that the actual value of t_{long} is not relevant and can be chosen within reasonable limits. For ease of measurement

we recommend a t_{long} of about 10 s which leads to relatively large remanence values, thereby increasing the accuracy of the technique.

Application of the tIRM technique to 11 loessic soil profiles from the Midwestern United States showed that the abundance of ultrafine magnetic grains is generally greater in soils that formed under humid climatic conditions.

ACKNOWLEDGMENTS

The authors would like to thank the numerous land owners for access and permission to sample, and the University of Nebraska School of Natural Resources for its generous support of our field work. Research at Trinity College was facilitated by a number of faculty research and travel grants. We would also like to thank Friedrich Heller and an anonymous reviewer for their constructive comments.

REFERENCES

- Banerjee, S.K., Hunt, C.P. & Liu, X.-M., 1993. Separation of local signals from the regional paleomonsoon record of the Chinese loess plateau: a rock-magnetic approach, *Geophys. Res. Lett.*, **20**, 843–846.
- Bettis, E.A., III, Muhs, D.R., Roberts, H.M. & Wintle, A.G., 2003. Last glacial loess in the conterminous USA, *Quat. Sci. Rev.*, **22**, 1907–1946.
- Bloemendal, J., King, J.W., Hall, F.R. & Doh, S.-H., 1992. Rock magnetism of Late Neogene and Pleistocene deep-sea sediments: relationship to sediment source, diagenetic processes, and sediment lithology, *J. Geophys. Res.*, **97**, 4361–4375.
- Dearing, J.A. & Jones, R.T., 2003. Supply and flux of sediment along hydrological pathways; research for the 21st century, *Global planet. Change*, **39**, 147–168.
- Dearing, J.A., Morton, R.I., Price, T.W. & Foster, I.D.L., 1986. Tracing movement of topsoil by magnetic measurements: two case studies, *Phys. Earth planet. Inter.*, **42**, 93–104.
- Dearing, J.A., Dann, R.J. L., Hay, K., Lees, J.A., Loveland, P.J., Maher, B.A. & O'Grady, K., 1996a. Frequency dependent susceptibility measurements of environmental materials, *Geophys. J. Int.*, **124**, 228–240.
- Dearing, J.A., Hay, K.L., Baban, S.M. J., Huddleston, A.S., Wellington, E.M. H. & Loveland, P.J., 1996b. Magnetic susceptibility of soil: an evaluation of conflicting theories using a national data set, *Geophys. J. Int.*, **127**, 728–734.
- Dearing, J.A., Brauer, A., Hu, Y., Doody, P. & James, P.A., 2001. Preliminary reconstruction of sediment-source linkages for the past 6000 yr at the petit lac d'annecy, france, based on mineral magnetic data, *J. Paleolimnol.*, **25**, 245–258.
- Deng, C., Liu, Q., Shaw, J., Zhu, R., Vidic, N.J., Verosub, K.L. & Singer, M.J., 2005. Mineral magnetic variation of the Jiaodao Chinese loess/paleosol sequence and its bearing on long-term climatic variability. *J. Geophys. Res.*, **110**, 1–17.
- Dunlop, D.J. & Özdemir, Ö., 1997. Rock magnetism, fundamentals and frontiers. Cambridge Univ. Press, Cambridge, New York.
- Forster, T., Evans, M.E. & Heller, F., 1994. The frequency dependence of low field susceptibility in loess sediments, *Geophys. J. Int.*, **118**, 636–642.
- Geiss, C.E. & Banerjee, S.K., 1997. A multi-parameter rock magnetic record of the last glacial-interglacial paleoclimate from south-central Illinois, USA, *Earth planet. Sci. Lett.*, **152**, 203–216.
- Geiss, C.E. & Zanner, C.W., 2007. Sediment magnetic signature of climate in modern loessic soils from the Great Plains. *Quat. Int.*, **162**, 97–110.
- Geiss, C.E., Umbanhowar, C.E., Camill, P. & Banerjee, S.K., 2003. Sediment magnetic properties reveal Holocene climate change along the Minnesota prairie-forest ecotone, *J. Paleolimnol.*, **30**, 151–166.
- Geiss, C.E., Zanner, C.W., Banerjee, S.K. & Minott, J., 2004. Signature of magnetic enhancement in a loessic soil in Nebraska, United States of America, *Earth planet. Sci. Lett.*, **228**, 355–367.
- Han, J., Lu, H., Wu, N. & Guo, Z., 1996. The magnetic susceptibility of modern soils in China and its use for paleoclimate reconstruction, *Stud. Geophys. Geodetica*, **40**, 262–275.
- Heller, F. & Evans, M.E., 1995. Loess magnetism, *Rev. Geophys.*, **33**, 211–240.
- Heller, F. & Liu, T.S., 1986. Paleoclimatic and sedimentary history from magnetic susceptibility of loess in China, *Geophys. Res. Lett.*, **13**, 1169–1172.
- Heller, F., Shen, C.D., Beer, J., Liu, T.S., Bronger, A., Suter, M. & Bonani, G., 1993. Quantitative estimates of pedogenic ferromagnetic mineral formation in Chinese loess and paleoclimatic implications, *Earth planet. Sci. Lett.*, **114**, 385–390.
- Hunt, C.P., Singer, M.J., Kletetschka, G., Ten Pas, J. & Verosub, K.L., 1995. Effect of citrate-bicarbonate-dithionite treatment on fine-grained magnetite and maghemite, *Earth planet. Sci. Lett.*, **130**, 87–94.
- Kletetschka, G. & Banerjee, S.K., 1995. Magnetic stratigraphy of Chinese loess as a record of natural fires, *Geophys. Res. Lett.*, **22**, 1241–1343.
- Kukla, G., Heller, F., Liu, X.M., Xu, T.C., Liu, T.S. & An, Z.S., 1988. Pleistocene climates in China dated by magnetic susceptibility. *Geology*, **16**, 811–814.
- Maher, B.A. & Taylor, R.M., 1988. Formation of ultrafine-grained magnetite in soils, *Nature*, **336**, 368–370.
- Maher, B.A. & Thompson, R., 1992. Paleoclimatic significance of the mineral magnetic record of the Chinese loess and paleosols, *Quat. Res.*, **37**, 155–170.
- Maher, B.A. & Thompson, R., 1999. *Quaternary climates, environments, and magnetism*, pp. 390. Cambridge University Press, New York.
- Maher, B.A., Thompson, R. & Zhou, L.P., 1994. Spatial and temporal reconstructions of changes in the Asian paleomonsoon: a new mineral-magnetic approach, *Earth planet. Sci. Lett.*, **125**, 461–471.
- Oches, E.A. & Banerjee, S.K., 1996. Rock-magnetic proxies of climate change from loess-paleosol sediments of the Czech Republic, *Stud. Geophys. Geodetica*, **40**, 287–300.
- Oldfield, F. et al., 2003. A high resolution late Holocene palaeo environmental record from the central Adriatic Sea, *Quat. Sci. Rev.*, **22**, 319–342.
- Porter, S.C., Hallet, B., Wu, X. & An, Z., 2001. Dependence of near-surface magnetic susceptibility on dust accumulation rate and precipitation on the Chinese loess plateau, *Quat. Res.*, **55**, 271–283.
- Reynolds, R.L. & King, J.W., 1995. Magnetic records of climate change. *Rev. Geophys.*, **33**, suppl. (IUGG Report), 101–110.
- Sartori, M., Tsatskin, A., Han, J.M., Evans, M.E. & Heller, F., 2005. The last glacial/interglacial cycle at two sites in the Chinese Loess Plateau: mineral magnetic, grain-size and 10Be measurements and estimates of palaeoprecipitation, *Palaeogeogr. Palaeoclimatol. Palaeoecol.*, **222**, 145–160.
- Singer, M.J., Verosub, K.L., Fine, P. & TenPas, J., 1996. A conceptual model for the enhancement of magnetic susceptibility in soils, *Quat. Int.*, **34–36**, 243–248.
- Spassov, S., Yue, L.P., Nourgaliev, D.K., Heller, F., Kretzschmar, R. & Evans, M.E., 2005. Detrital and pedogenic magnetic mineral phases in the loess/paleosol sequence at Lingtai (Central Chinese Loess Plateau), *Phys. Earth planet. Inter.*, **140**, 255–275.
- Vidic, N.J., TenPas, J.D., Verosub, K.L. & Singer, M.J., 2000. Separation of pedogenic and lithogenic components of magnetic susceptibility in the Chinese loess/paleosol sequence as determined by the CBD procedure and a mixing analysis, *Geophys. J. Int.*, **142**, 551–562.
- Worm, H.-U., 1998. On the superparamagnetic-stable single domain transition for magnetite, and frequency dependence of susceptibility, *Geophys. J. Int.*, **133**, 201–206.
- Worm, H.U., 1999. Time dependent IRM: a new technique for magnetic granulometry, *Geophys. Res. Lett.*, **26**, 2557–2560.